ELSEVIER

Polymer 42 (2001) 8153–8161

polymer

www.elsevier.nl/locate/polymer

Light transmission of composites made from the biaxially drawn ultrahigh molecular weight polyethylene (UHMWPE) film and polyether polyurethane

Zheng Gui Tang*, Swee Hin Teoh

Laboratory for Biomedical Engineering, Department of Mechanical Engineering, Institute of Engineering Science, Centre for Biomedical Materials Applications and Technology, National University of Singapore, 10 Kent Ridge Crescent, Singapore 119260

Received 7 November 2000; received in revised form 10 April 2001; accepted 20 April 2001

Abstract

Optically transparent composite membranes have been made from two immiscible polymers, the biaxially drawn UHMWPE (the fiber, 80–400 μm in diameter) and the polyether polyurethane. The as-made composites have a volume fraction up to 24% and a light transparency up to 70%. The light transmission of all the composites tested is linearly dependent on the wavelength of the visible incident light. The slope (K) and the constant (C) derived from the linear relation were correlated with a mathematical model. The K-value changed with the changed of the residual voids in the composite. The C-value changed with the change of the refractive indices. The light transmission of the composite membranes can be optimized through the control of both K and C, preferably controlling the K-values. The highest light transparency was found in Toyobo TM5 composite heat compacted at 115°C.

Keywords: Light transmission; Nano-fiber UHMWPE composites; Heat compaction

1. Introduction

Transparent composites can be made from two transparent materials such as glass fiber and poly(methyl methacrylate) (PMMA) [1]. The light scattering between two materials was controlled by closely matching the refractive indices of PMMA and glass fibers. More than 80% light transparency was achieved through hot pressing the laminated PMMA and glass fiber stacks. The light transmission is governed by the mismatch of the refractive indices of reinforcement and matrix materials $(n_f - n_p)^2$ and the volume content of reinforcement fibers (V_f). A continuous study of the aging behavior of this composite [2] revealed the contribution of volume fraction and radius of the gas bubbles to the light transparency ($V_{f,b}/R_b$). The temperature–aging cast a great impact on the light transparency of the composite, resulting in significant loss of light transparency from 96 to 39% when it was hot pressed at 100°C for 18 h.

The temperature and wavelength dependence of the light transmission through the glass fibers and PMMA composite was reported [3,4]. This is due to the temperature and wavelength dependence of the refractive indices of both reinforcement fibers and matrix materials. Annealing of glass fibers was therefore taken into account in matching the refractive index with that of PMMA [5]. The as-made glass fiber PMMA composite can be made to have a light transparency progressively close to that of the pure PMMA sheet.

The concept of making transparent composites can be extended to different types of glass fibers and matrix materials. A transparent fluorophosphate glass fiber reinforced poly(chlorotrifluoroethylene) (PCTFE) composite was therefore developed [6]. Fluorophosphate glass fibers were deliberately made to matching the matrix material of PCTFE ($n_D = 1.425$). Tang and co-workers [7,8] made a transparent composite using biaxially drawn ultrahigh molecular weight polyethylene (UHMWPE) and polyether urethane. Both fibrous UHMWPE and polyurethane were inter-woven in an inter-connected network, which improved the thermal stability of the biaxially drawn UHMWPE [9]. The heat compaction of the as-made composite near the melting temperature showed an interesting change of the light transmission. This attracts our attention for the light transmission properties of the polyurethane reinforced with biaxially drawn UHMWPE. In this paper, the light

* Corresponding author. Corresponding address: Blk359, #10-311, Clementi Avenue 2, Singapore 120359. Tel.: +65-793-8582/872-2565; fax: +65-793-5362.

E-mail address: zgtang@gintic.gov.sg (Z.G. Tang).

0032-3861/01/$ - see front matter
PII: S0032-3861(01)00304-4

transmission of the as-made composites will be presented. The fiber diameter will be evaluated in scanning electron microscope (SEM). A series of heat compaction will be conducted and evaluated for their effects on the light transmission of the composites. The light transmission properties of the composites will be discussed in correlation with the microstructural changes of the composites during the heat compaction process.

2. Experimental

2.1. Sample preparation

The composite membranes were made from biaxially drawn UHMWPE film (Solupor TM 7P03, DSM, The Netherlands, about 75% porosity) and polyether polyurethane materials (Toyobo TM5, Toyobo, Japan and Tecoflex 80A, Thermedics, Woburn, USA) following the methods in our previous publications [8,9]. Briefly, the porous biaxially drawn UHMWPE films, Solupor TM 7P03 was impregnated in 10% Toyobo TM5/*N*,*N*-dimethyl formaldehyde (DMF) solution and 10% Tecoflex 80A/tetrahydrofuran (THF) solution for about 3 days and then dried in vacuum to remove the solvent. A translucent composite membrane was therefore obtained. The composite was sandwiched in two Teflon sheets and heat compacted in Laboratory Press (LABQUIP Model LP 50, Lab Tech Engineering) under about 18 MPa at temperature of 95, 105, 115, 125, and 135°C for about 1.5 h. The heat compaction temperature was recorded by inserting a thermocouple inside the Teflon sheets and reading it with a display (T-Copper Constantan Model 199, Omega). The heat compaction temperature was controlled precisely within a deviation of 1°C. The heat compacted membrane (HCM) was removed from the Teflon sheets upon cooling to the room temperature. The sample membranes were placed in a sealed plastic bag and conditioned for a week before specific evaluation.

2.2. Thickness measurement

The thickness of HCM was measured using a modified surface contact method [8]. The sample membrane was sandwiched between a standard stage and metal plate (1.000 mm standard). The measurement was carried out on a one point contact instrument (Cary Compar B), which usually was used to measure the thickness of metallic materials. The thickness of HCM was read indirectly after subtracting 1.000 mm of the standard metal plate.

2.3. Reinforcement fraction

Samples of the composite membranes were cut into 10 mm × 10 mm square. They were weighed before and after impregnated in solvent and dried under vacuum. In this study, DMF was used to remove the Toyobo TM5 polyurethane while THF was used to remove the Tecoflex 80A polyurethane. This method is adopted in conventional composite evaluation [10], assuming the deformation of the reinforcement has no significant effects on the evaluation. The porous UHMWPE film of the same size was cut and used for control and evaluation of the possible cross-linkage and other chemical interaction. The reinforcement fraction was calculated through the following equations:

$$\text{Reinforcement weight fraction (w/w)} = (W_f/W_c) \times 100\%,$$

$$\text{Reinforcement volume fraction (v/v)} = [W_f\rho_m/(W_f\rho_m + W_m\rho_f)] \times 100\%$$

where W_f is the weight of the porous UHMWPE films, W_c the weight of the composite membranes, W_m the weight of the matrix polyurethane, ρ_f the density of the UHMWPE (~0.96), and ρ_m the density of the polyurethane (~1.20) [11].

2.4. Scanning electron microscopy

Specimens of the porous UHMWPE films were coated with gold for morphological observations. Pictures were taken from the SEM machine (Jeol JSM-T330 scanning microscope). The working voltage used was 5 kV. Lower voltage is encouraged for the preservation of fine details of UHMWPE [12].

2.5. Light transmission

Light transmission tests were carried out on U-3410 Spectrophotometer (Hitachi). The aperture for light transmission is 20 mm × 10 mm. Spectra of light transmission were scanned in the wavelength range from 350 to 800 nm. Samples tested were the porous UHMWPE, composite membranes and heat compacted composites.

3. Results

3.1. Thickness and reinforcement fraction

Results of the thickness are listed in Table 1 for the biaxially drawn UHMWPE films, the composite membranes, and the HCMs. Heat compaction significantly reduced the thickness of the porous UHMWPE films, resulting in shrinkage of more than half of the thickness. The

Table 1
Thickness of the drawn UHMWPE films (BD-UHMWPE), polyurethane films, and composite membranes (with and without heat compaction) ($n = 5$)

Compaction temperature (°C)	BD-UHMWPE film (μm)	Toyobo TM5 CM (μm)	Tecoflex 80A CM (μm)
25	33.6 ± 2.5	38.2 ± 5.6	74.0 ± 8.2
95	16.3 ± 1.4	33.2 ± 3.3	62.7 ± 4.5
125	13.2 ± 1.0	29.3 ± 2.8	59.2 ± 3.8

Table 2
Reinforcement fractions of the composite membranes (weight of the BD-UHMWPE film is 0.68 ± 0.07 ($n = 5$))

Material	W_c (mg)	W_f (mg)	Weight fraction (w/w)	Volume fraction (v/v)
Toyobo TM5 CM	4.83 ± 0.35 ($n = 7$)	0.77 ± 0.05 ($n = 7$)	15.9 ± 1.5	19.16 ± 1.4
Heat compacted Toyobo TM 5 CM[a]	3.38 ± 0.18 ($n = 9$)	0.68 ± 0.07 ($n = 8$)	20.1 ± 2.9	23.94 ± 2.7
Tecoflex 80A CM	5.75 ± 0.50 ($n = 8$)	0.68 ± 0.11 ($n = 8$)	11.8 ± 2.7	14.36 ± 2.8
Heat compacted Tecoflex 80A CM[b]	5.68 ± 0.40 ($n = 8$)	0.70 ± 0.11 ($n = 8$)	12.3 ± 2.7	14.94 ± 2.8

[a] Heat compaction temperature at 125°C.
[b] Heat compaction temperature at 95°C.

infiltration of Toyobo TM5 and Tecoflex 80A significantly reduced the effects of compression.

Table 2 shows the reinforcement fractions of the composite membranes. The weight fraction lies in the range of 10.0–21.0% while the volume fraction lies in the range of 14.0–24%. The Toyobo TM5 CM had the higher reinforcement fraction compared to the Tecoflex 80A CM.

3.2. The SEM morphology of the porous biaxially drawn UHMWPE

Fig. 1 shows the surface morphology of the porous biaxially drawn UHMWPE membranes (BD-UHMWPE). Pores of a diameter less than 100 μm were observed on the surface of the BD-UHMWPE (Fig. 1a). These pores were randomly distributed and non-spherical. All the pores were inter-connected and formed in layers of porous UHMWPE. In a single surface layer, the pore sizes could be as big as 100 μm. Due to the scattering of light, stress whitened regions were observed in the BD-UHMWPE surface. At high magnification, two discernible components, microfibril bundles (M-B) and microfibril networks (M-N), were clearly seen (Fig. 1b). The microfibril bundles formed the structural skeletons of the individual layers. A much closer view revealed the fine structures of the microfibril bundles and the adjunct microfibrils (Fig. 1c). Microfibril bundles were composed of fibers with a diameter of about 400 nm; while the microfibrils were approximately 80 nm in diameter. The average pore size of the fine pores was observed to be less than 1 μm.

Fig. 2 shows that the majority of pores had dimensions in the range 0.1–0.5 μm. This agrees with the data (0.2–0.4 μm), measured by the supplier, using the Coulter method (ASTM E1294-89), which was provided by DSM.

3.3. Light transmission

Fig. 3 shows the light transmission of the porous UHMWPE, polyurethane and composite membranes. The porous UHMWPE films were opaque and no light was transmitted because the light was scattered by the porous structures. Polyurethane films, made from Tecoflex 80A and Toyobo TM5 by solution casting, were transparent and had a light transmission rate that ranged from 60 to 90%. The composite membranes, made by solution casting polyurethane on the porous UHMWPE films were translucent and had a light transmission rate from 2 to 30%. Theoretically, the rate of light transmitted is inversely proportional to the thickness of the membranes. Tecoflex 80A films have a lower rate of light transmission than Toyobo TM5 films. This indicated that the thickness governed the change in light transmission. However, the same phenomena could not be seen in the composite membranes. Tecoflex 80A composite membranes have a higher light transmission than Toyobo TM5 composite membranes.

Fig. 4 shows the light transmission of the heat compacted UHMWPE films. When heat compacted at 95°C, the porous UHMWPE films became partially translucent and the light transmission rate was approximately 1%. The increased light transmission was largely due to the reduction of the porosity in the heat compacted films. The light transmission was increased up to 40% when the porous UHMWPE films were heat compacted at 105°C. This value remained unchanged for the UHMWPE films heat compacted up to a temperature of 125°C. The light transmission was further improved in samples heat compacted at 135°C. The maximum light transmission measured was approximately 60%.

Fig. 5 shows the light transmission in Toyobo TM5 composite membranes. When samples were heat compacted at 95°C, the light transmission rate increased up to 10%, in comparison to that in the corresponding heat compacted UHMWPE films. With the increase of the heat compaction temperature, the light transmission of the heat compacted composites was significantly improved. The highest transmission rate was approximately 70% in samples heat compacted at 115°C. At a heat compaction temperature of 125°C, the light transmission rate decreased to approximately 40% and at 135°C to 20%.

Fig. 6 shows the light transmission in Tecoflex 80A composite membranes and heat compacted derivatives. Tecoflex 80A composite membranes had a light transmission approximately 20% higher than Toyobo TM5 composite membranes. When Tecoflex 80A composites were heat compacted at 95°C, the light transmission increased up to approximately 40% due to the removal

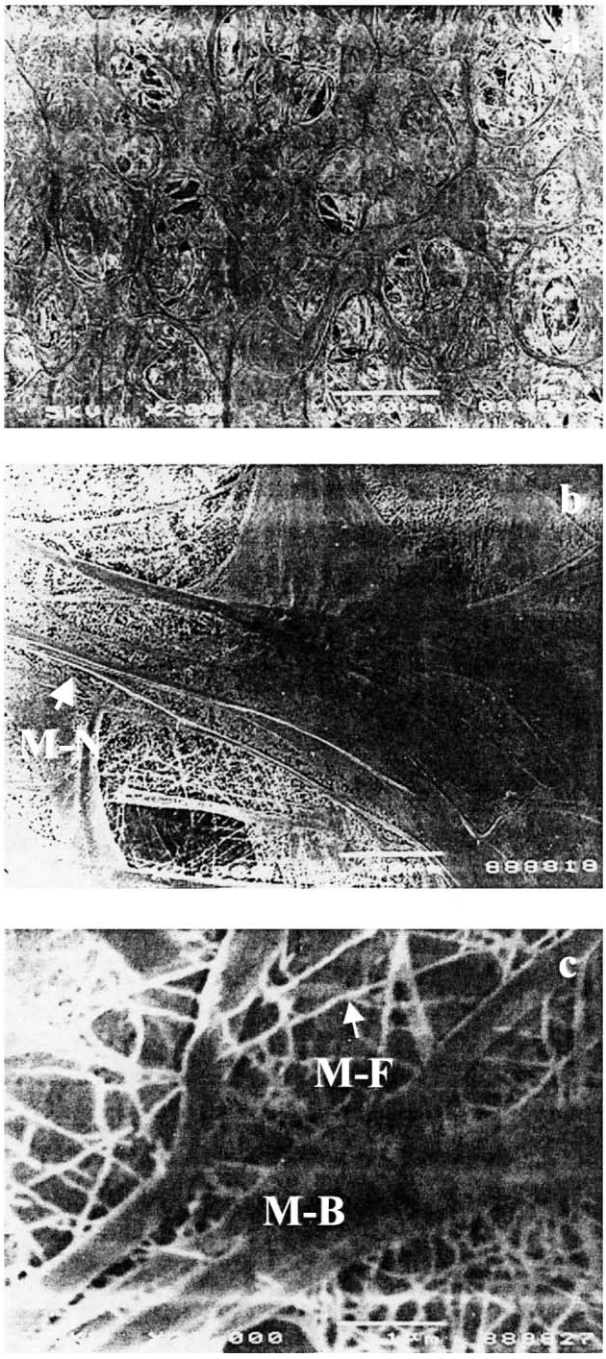

Fig. 1. (a) Porous structures of the biaxially drawn UHMWPE membranes; (b) microfibril bundles (M-B) and microfibril network (M-N); (c) microfibrils (M-F) and microfibril bundle (M-B).

of the voids in Tecoflex 80A composites. The light transmission of the heat compacted Tecoflex 80A composites was found to be non-linear with respect to the increase of the heat compaction temperature. Heat compaction at 105°C rendered Tecoflex 80A less transparent. When Tecoflex 80A composites were heat compacted at 115°C, the light transmission was increased again. It was relatively stable in samples heat compacted from 115 to 125°C, and slightly decreased in samples heat compacted at 135°C.

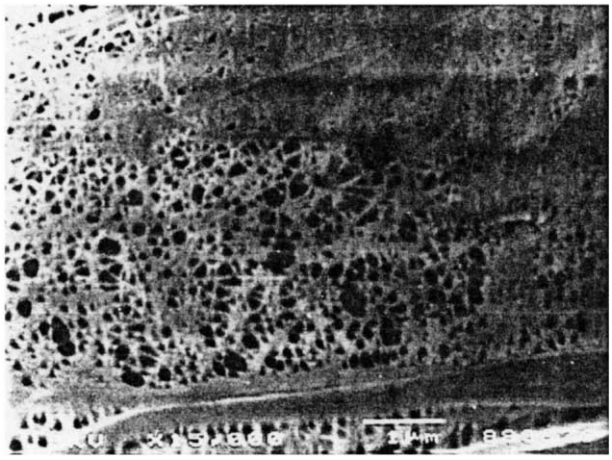

Fig. 2. Microfibril structures of the porous UHMWPE membranes.

4. Discussion

The light transmission of the composite membranes is governed by the mismatch of the refractive indices of reinforcement fibers and matrix materials [1], the volume content of reinforcement fibers [1], and the volume fraction and radius of the gas bubbles [2]. The refractive index is strongly dependent on temperature, annealing, and wavelength of the light used for evaluation [4,5]. The compression on the porous UHMWPE films did not significantly change the reinforcement fibers but the volume fraction of the voids especially the voids among the laminar layers. Infiltration did the same by filling the voids with polyurethane. This tells why the composite did not reduce its thickness as significantly as the porous UHMWPE film. If the process was divided into evaporation, compression, and annealing, the voids in the composite membranes were largely removed through evaporation and compression (Fig. 7). The transparency of the as-made composite membranes was therefore introduced.

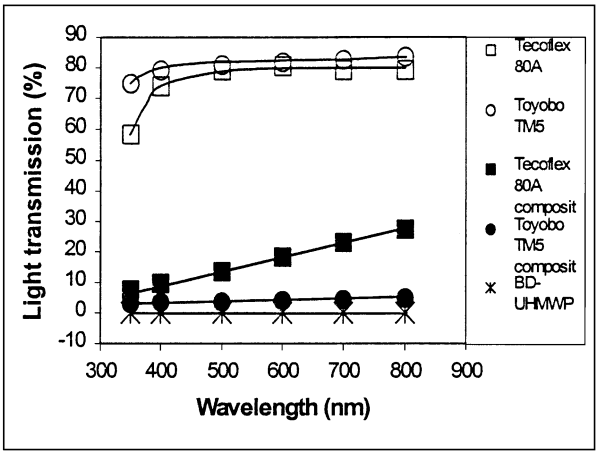

Fig. 3. The light transmission rate of the porous biaxially drawn UHMWPE membrane, Toyobo TM5 and its composite, Tecoflex 80A and its composite.

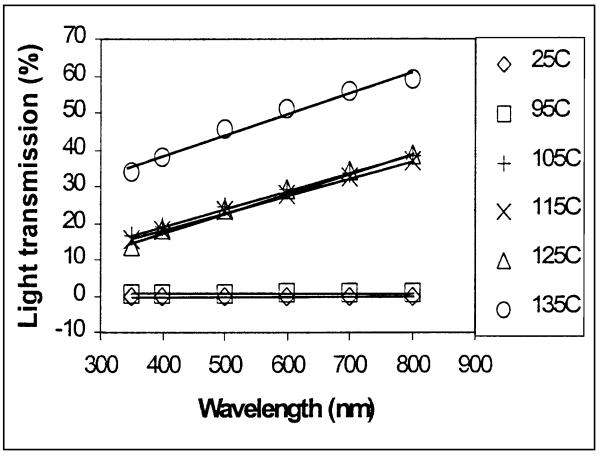

Fig. 4. The light transmission rate of the porous biaxially drawn UHMWPE membranes and their heat compacted derivatives.

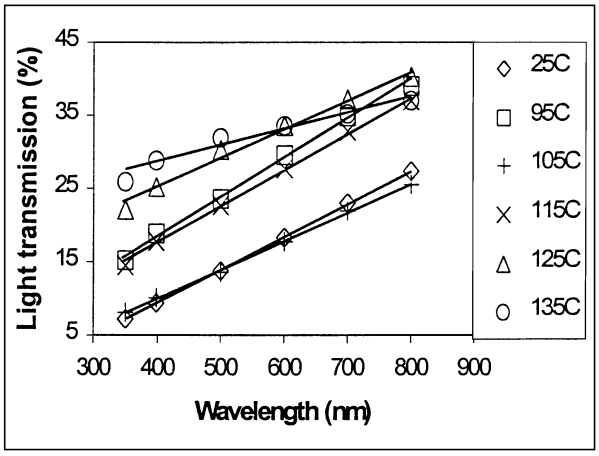

Fig. 6. The light transmission rate of the Tecoflex 80A composite membranes and their heat compacted derivatives.

The light transmission of the porous UHMWPE films, polyurethane composites, and their heat compacted samples tested was dependent on the wavelength of the incident light. This could be described as

$$T\% = K\lambda + C \tag{1}$$

The K- and C-values for the specific samples are depicted in Figs. 8–10. According to the thermal history of UHMWPE, heat compaction up to 95°C would not significantly affect UHMWPE molecules. The UHMWPE fibers were considered to be intact at 95°C [13,14]. The change of the light transmission between samples heat compacted at 95°C and samples without heat compaction can be estimated through Eq. (2) [15] (See Appendix A for details).

$$\Delta T_I = T_{95} - T_{25} = (A_{95} - A_{25}) + AB_0(\Delta m^2/\lambda_0^2)(h_{25} - h_{95}) + 3A\{[h_{25}(V_{f,b}/D_b)_{25}] - [h_{95}(V_{f,b}/(D_b)_{95}]\} \tag{2}$$

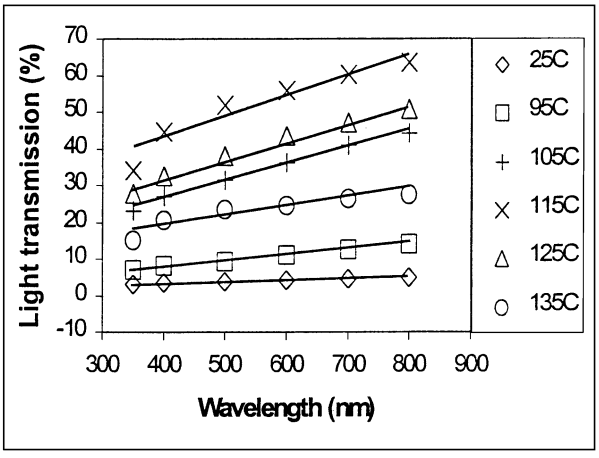

Fig. 5. The light transmission rate in the Toyobo TM5 composite membranes and their heat compacted derivatives.

where A is a constant from I_x, $B_0 = 8\pi D_f V_{f,m}$ derived from the estimation of the scattering efficiency (Q) (See Appendix A), Δm the mismatch of the refractive index, h the thickness of the sample, $V_{f,b}$ the volume fraction of the fiber, and D_b the diameter of the gas bubble.

If $(A_{95} - A_{25}) = 0$, and $h_{95}/h_{25} = k$, the equation can be simplified as

$$\Delta T_I = T_{95} - T_{25} = M(1-k) + N\{[(V_{f,b}/D_b)_{25}] - [k(V_{f,b}/(D_b)_{95}]\} \tag{3}$$

where $M = AB_0h_{25}(\Delta m^2/\lambda_0^2)$, $\Delta m^2 = (m_1 - m_2)^2$, and $N = 3Ah_{25}$.

The change of the light transmission in the heat compacted UHMWPE film was due to the change in thickness (h) and void content ($V_{f,b}/D_b$). Based on the experimental data, ΔT_I was close to zero. Eq. (3) can be rewritten as

$$k = [(M/N) + (V_{f,b}/D_b)_{25}]/[(M/N) + (V_{f,b}/D_b)_{95}] \tag{4}$$

If $(V_{f,b}/D_b)_{95}$ is larger than $(V_{f,b}/D_b)_{25}$, k will be less than 1. In practice, heat compaction, k is approximately 0.5. The volume fraction of the voids is also reduced after heat compaction. Therefore, the diameter of the voids is the primary parameter controlled by the heat compaction process up to 95°C.

When the porous UHMWPE film was heat compacted up

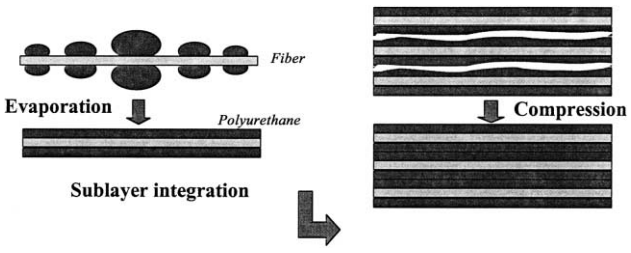

Fig. 7. Schematic diagrams of the evaporation and compression during the composite fabrication.

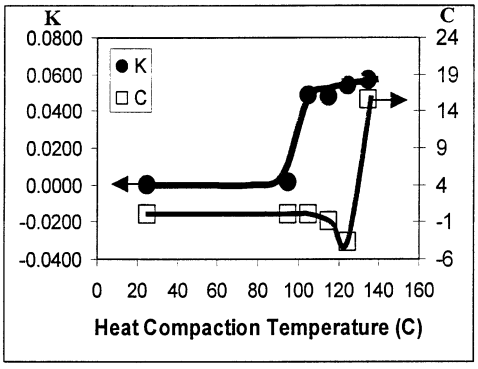

Fig. 8. Temperature profiles of *K*- and *C*-values in porous biaxially drawn UHMWPE membranes and their heat compacted derivatives.

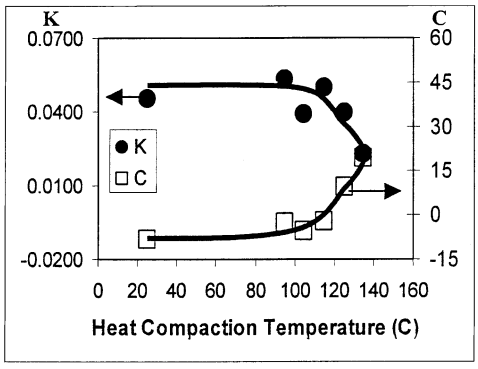

Fig. 10. Temperature profiles of *K*- and *C*-values in Tecoflex 80A composite membranes and their heat compacted derivatives.

to 105°C, the light transmission of the compacted UHMWPE films increased significantly up to approximately 40%. The change in light transmission can be expressed as follows (Eq. (5)) in view of the constant thickness of the UHMWPE film during the heat compaction from 95 to 105°C.

$$\Delta T_{II} \approx A_{II}[(m_1 - m_2)^2_{95} - (m_1 - m_2)^2_{105}] + B_{II}\{(V_{f,b}/D_b)_{95} - [V_{f,b}/(D_b)]_{105}\} \quad (5)$$

where $A_{II} = AB_0h_{95}/(\lambda_0^2)$ and $B_{II} = 3A_0h_{95}$.

Considering there was no significant change in the size of voids (D_b), the light transmission increase was mainly due to the filling of the voids by the matrix UHMWPE [14,16–18].

$$\Delta T_{II} \approx A_{II}[(m_1 - m_2)^2_{95} - (m_1 - m_2)^2_{105}] + [B_{II}/(D_b)_{95}]\{(V_{f,b})_{95} - (V_{f,b})_{105}\} \quad (6)$$

or in case $(V_{f,b})_{105} = 0$

$$\Delta T_{II} \approx A_{II}[(m_1 - m_2)^2_{95} - (m_1 - m_2)^2_{105}] + [B_{II}/(D_b)_{95}](V_{f,b})_{95} \quad (7)$$

The increase in K_{95-105} value was strong evidence for the thermal fusion of voids $(V_{f,b})_{95}$ by the matrix UHMWPE in heat compacted UHMWPE films. This is because the C_{95-105} value that did not show significant changes after heat compaction. Therefore, the *K*-value can be linked to the removal of residue voids resulting in the change of the refractive index of the matrix materials, such as amorphous UHMWPE in the reinforcement materials.

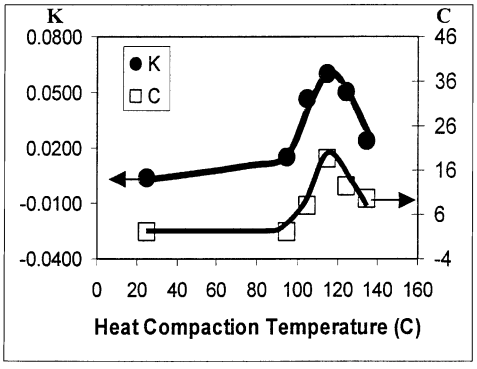

Fig. 9. Temperature profiles of *K*- and *C*-values in Toyobo TM5 composite membranes and their heat compacted derivatives.

When the porous UHMWPE film was heat compacted from 105 to 125°C, no significant change in thickness was observed. The experimental data also showed that ΔT_{III} was about zero.

The porous UHMWPE film underwent a significant change in morphology when it was heat compacted from 125 to 135°C [14,16–18]. The process parameter associated with this change was the *C*-value and the light transmission. The correlation of the *C*-value with the change in microstructures was considered likely in view of the insignificant change in the *K*-value at a high heat compaction temperature.

Heat compaction at 135°C transformed the UHMWPE fibers into a homogeneous UHMWPE. Therefore, the light transmission can be written as

$$\Delta T_{IV} \approx A_{IV}(m_1 - m_2)^2_{125} - A^{\#}_{IV}(m_1 - m_2)^2_{135} \quad (8)$$

where $A_{IV} = [AB_0h_{125}/(\lambda_0^2)]_{125}$ and $A^{\#}_{IV} = [AB_0h_{135}/(\lambda_0^2)]_{135}$.

If the UHMWPE fibers were considered as almost melted, e.g. $(m_1 - m_2)_{135} \approx 0$, Eq. (8) can be written as

$$\Delta T_{IV} \approx A_{IV}(m_1 - m_2)^2_{125} \quad (9)$$

The change in *C*-value was associated with the change of the refractive index of crystalline UHMWPE fibers or the mutual changes in refractive indices between both reinforcement and matrix materials (Eq. (9)).

The above discussions showed that the K_T was directly associated with the filling of the voids by partially melting the UHMWPE. This resulted in a significant change in the average diameter (D_b) of the voids and their volume fraction ($V_{f,b}$). The C_T was closely related to the disorientation of the crystalline UHMWPE fibers or the change of the mismatching in refractive indices between matrix materials (m_1) and the reinforcement materials (m_2).

The differences between Figs. 8 and 9 are twofold.

Firstly, the *K*-value has a maximal value in samples heat compacted at 115°C. As it was discussed for the porous UHMWPE film, the increase of the *K*-value is an indication of the filling of the voids with the matrix material. The maximal *K*-value indicates that the polyurethane and UHMWPE are not miscible when the composite is heat compacted above 115°C. Segregation of the mobile UHMWPE and the mobile Toyobo TM5 may be responsible for the decrease of the *K*-value. Secondly, the *C*-value also has a maximal value in samples heat compacted at 115°C. This indicates that the mobile UHMWPE has a good refractive index match with its environment — the crystalline UHMWPE fibers and the Toyobo TM5. However, the *C*-value decreases in samples heat compacted above 115°C. This did not happen in the porous UHMWPE film. This phenomenon is due to the matrix polyurethane, which is mobilized by the mobile UHMWPE. It increases the mismatching of the refractive indices between the UHMWPE fibers and the matrix materials as the matrix materials are comprised of the immiscible Toyobo TM5 and the UHMWPE.

Based on the discussion, the optimum temperature for heat compaction of the Toyobo TM5 composite membranes could be 115°C. Heat compaction at this temperature resulted in the least void content and the least microstructure changes.

Fig. 10 shows that Tecoflex 80A is completely different from Toyobo TM5 and also UHMWPE. The Tecoflex 80A appears quite compatible with the mobile UHMWPE in composite samples heat compacted up to 95°C. Heat compaction slightly increases the *K*-value. However, this cannot be sustained for samples heat compacted above 95°C.

The *K*-value of the Tecoflex 80A composite decreases when it is heat compacted at temperatures from 95 to 135°C. This suggests that Tecoflex 80A may be also immiscible with the UHMWPE when it was heat compacted above 95°C.

Interestingly, the *C*-value shows that the refractive index of the Tecoflex 80A appears to show a reasonable match with the UHMWPE when the composite is heat compacted above 95°C. Tecoflex 80A may align along the UHMWPE fibers' orientation but is probably highly immiscible. This hypothesis was supported by the extrusion of the UHMWPE from the composite heat compacted at 135°C and also the transformation of the UHMWPE fibers from biaxial to uniaxial orientation in samples heat compacted at 115°C [15].

In general, Tecoflex 80A composites could be solidified through heat compaction. The optimum temperature for heat compaction was at around 95°C. This indicated that UHMWPE fibers were not as temperature resistant in Tecoflex 80A composites as compared with the fibers in Toyobo TM5 composites.

5. Conclusions

The light transmission of the solution cast polyurethane composites was correlated with the physical and thermal properties of the reinforcement UHMWPE fibers through qualitative mathematical model. The UHMWPE fibers lie in the range of the wavelength of the visible light. The impregnation and heat compaction made it possible to fabricate transparent composite membranes from UHMWPE and polyurethane. The light transmission study of these composites provided the following points that might help for the understanding of the interaction of two immiscible polymers.

1. Composites of UHMWPE fibers and polyurethane were transparent. The transparency of the composite membranes increased linearly with the increase of the wavelength. This differs from the transparent polyurethane films that give a large deviation when linear relation was placed on them.
2. The *K*-value is closely associated with the change of the void content of the composites. An increase of the *K*-value indicated thermal fusion of the voids while a decrease of the *K*-value represented void formation due to the repulsion between polyurethane and UHMWPE fibers.
3. The *C*-value is related to the interaction between the polyurethane matrix and the UHMWPE reinforcement materials. It is primarily associated with the change of the reinforcement materials. The increase in the *C*-value indicated that the refractive index matching layers were formed between two immiscible materials while the decrease in the value of *C* represented the repulsion between two immiscible materials.
4. The combination of *K*- and *C*-values gives a primary guideline for the optimization of the void content and component interaction by applying heat compaction.
5. The optimum heat compaction temperature for a Tecoflex 80A composite is around 95°C and for a Toyobo TM5 composite is approximately 115°C.

Acknowledgements

The authors would like to thank Professor Mitsuo Umezu, Waseda University, for his help in getting the Toyobo TM5 materials. The authors also would like to acknowledge Dr Tung Siew Kung, Materials Science Division, Department of Mechanical and Productional Engineering for his endless support and assistance in obtaining high quality SEM photographs.

Appendix A. Theoretical consideration for light transmission

When an incident beam of intensity I_0 traverses a slab of particles over an optical path of length x, assuming multiple scattering can be neglected and there is no change in the

phase and wavelength of the light after scattering the transmitted\quad intensity, I_x, is given by Eq. (A1) (Fig. A1) (Willmouth, 1986)

$$I_x = AI_0 \exp(-NCx) \tag{A1}$$

where the A is a constant, N the number of scattering particles per unit volume, and C the scattering cross-section per particle

When $x = h$, the thickness of the slab, then I_t can be expressed as

$$I_t = AI_0 \exp(-NCh) \tag{A2}$$

Here, the number density N can be calculated from the diameter D and volume fraction V of spheres. Thus,

$$N = 6V/\pi D^3 \tag{A3}$$

According to the Mie theory, the scattering cross-section C is given by

$$C = (\lambda_0^2/2m_2\pi)\sum(2n + 1)(|a_n|^2 + |b_n|^2) \tag{A4}$$

The a_n and b_n are functions of relative refractive index, $m = m_1/m_2$, free space wavelength, λ_0, diameter of the spheres and refractive index, m_1 for spheres and m_2 for matrix, respectively. It can be simplified as

$$C = (\lambda_0^2/2m_2\pi)f(m, m_2, m_1, \lambda_0, D) \tag{A5}$$

The light transmission rate, T, therefore can be calculated from Eq. (A6).

$$T = I_t/I_0 = A \exp[-Bf(m, m_2, m_1, \lambda_0, D)] \tag{A6}$$

Here $B = [(3\lambda_0^2 Vh)/(m_2\pi^2 D^3)]$.

When the incident light goes through a thin film of composites, the light transmission rate can be similarly estimated from Eq. (A6) (van de Hulst, 1957), but N will be expressed as

$$N = V/v \tag{A7}$$

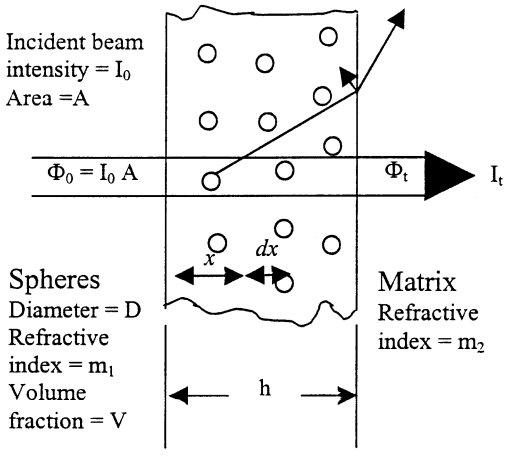

Fig. A1. Microstructural model used to calculate transparency parameters from Willmouth FM. In: Meeten GH, editor. Optical properties of polymers; 1986.

According to Lin et al. [2], the scattering cross-section, C is related to the scattering efficiency, $Q = C/G$, where G is the geometrical cross-section which is D per unit length for an infinite cylinder of diameter, D. The light transmission rate, T will be written as

$$T = I_t/I_0 = A \exp\Big[-\sum 4VhQ/\pi D\Big] \tag{A8}$$

This model worked quite well for glass fiber reinforced PMMA composites [2]. The model predicted that the important factors affecting the optical transmission are the fiber diameter, fiber volume content, thickness of the composites and the scattering effects in bulk materials. When the fibers were selected, the thickness (h) and the scattering efficiency (Q) will be the major parameters affecting the light transmission in composites in case there are no significant changes in volume fraction and fiber diameter. The scattering usually happens in the presence of the heterogeneous phases like fibers and voids in the matrix materials, which usually have distinct characteristic refractive indices. Lin et al. [2] considered the effects of the voids in the presence of composite membranes. The light transmission rate was rewritten as

$$T = A \exp\Big\{\Big[-\sum 4V_{f,m}hQ_f/\pi D_f\Big] + \Big[-\sum 3V_{f,b}hQ_b/2D_b\Big]\Big\} \tag{A9}$$

where Q_f and Q_b are the scattering efficiency of the fibers and gas bubbles, respectively. For large spheres of bubbles, Q_b is approximately 2.0. The Eq. (A9) can be simplified as

$$T = A \exp\Big\{\Big[-\sum 4V_{f,m}hQ_f/\pi D_f\Big] + \Big[-\sum 3V_{f,b}h/D_b\Big]\Big\} \tag{A10}$$

Deducing Q_f from Eq. (A10) is still mathematically complex. So in the case of small refractive index mismatching and $D_f < 100$ nm (Rayleigh scattering theory), an empirical scattering efficiency factor Q_f can be introduced (Eq. (A11)) to simplify the mathematics.

$$Q_f \propto (\Delta m/m_2)^2 \approx B(\Delta m/m_2)^2 \tag{A11}$$

Here B is a constant for the estimation of Q_f in Eq. (A11). The light transmission rate T can be roughly estimated through Eq. (A12)

$$T = A \exp\Big\{\Big[-\sum(4V_{f,m}hB)(m_1 - m_2)2/\pi m_2^2 D_f\Big] + \Big[-\sum 3V_{f,b}h/D_b\Big]\Big\} \tag{A12}$$

Similar estimation was made in approximating Q_f in Eq. (A13).

$$Q_f = 2 - (4/\rho)\sin\rho + (4/\rho^2)(1 - \cos\rho) \tag{A13}$$

Here

$$\rho = 2\alpha(m - 1) = (2\pi D/\lambda_0)(m_1 - m_2)$$

If the mismatching of $(m_1 - m_2)$ is small, Q_f can be simplified as

$$Q_f \approx [2\pi^2 D_f^2 (m_1 - m_2)^2]/\lambda_0^2] \quad \text{(A14)}$$

Combining Eqs. (A10) and (A14), the light transmission rate T can be estimated through Eq. (A15).

$$T = A \exp\left\{\left[-\sum (8\pi D_f V_{f,m} h (m_1 - m_2)^2/\lambda_0^2 \right] + \left[-\sum 3V_{f,b} h/D_b \right]\right\} \quad \text{(A15)}$$

or

$$T = A \exp\left\{\left[-\sum B_0 h (m_1 - m_2)^2/\lambda_0^2 \right] + \left[-\sum (3V_{f,b} h)/D_b \right]\right\} \quad \text{(A16)}$$

where $B_0 = 8\pi D_f V_{f,m}$. The light transmission rate can be further simplified through first grade approximation of Eq. (A16).

$$T = A - AB_0 h (m_1 - m_2)^2/\lambda_0^2 - (3AV_{f,b} h)/D_b \quad \text{(A17)}$$

or

$$T = A_0 - A_1 (m_1 - m_2)^2/\lambda_0^2 - A_2 V_{f,b}/D_b \quad \text{(A18)}$$

where $A_0 = A$, $A_1 = AB_0 h$, and $A_2 = 3Ah$. If we consider the orientation of biaxially drawn fibers in our reinforcement materials, Eq. (A18) could be expressed as

$$T = A_0 - A_1 [\alpha (m_{f1} - m_2)^2 + \beta (m_{f2} - m_2)^2]/\lambda_0^2 - A_2 V_{f,b}/D_b \quad \text{(A19)}$$

where α and β are factors used to adjust the contribution of the mismatching between oriented fibers (m_{f1} and m_{f2}) and the polyurethane matrix (m_2).

References

[1] Lin H, Day DE, Stoffer JO. Polym Engng Sci 1992;32(5):344–50.
[2] Lin H, Day DE, Stoffer JO. Polym Compos 1993;14(5):402–9.
[3] Lin H, Day DE, Weaver KD, Stoffer JO. J Mater Sci 1994;29:5193–8.
[4] Kang S, Day DE, Stoffer JO. J Non-Cryst Solids 1997;220:299–308.
[5] Kang S, Lin H, Day DE, Stoffer JO. J Mater Res 1997;12(4):1091–101.
[6] Dechent WL, Lin H, Day DE, Stoffer JO. Abstr Pap Am Chem, 14-PMSE, Part 2 1993;S205:26–27.
[7] Tang ZG, Ramakrishna S, Teoh SH. In: Proceedings of the Ninth International Conference on Biomedical Engineering, 1997 December 3–6; Singapore. p. 563–4.
[8] Teoh SH, Tang ZG, Ramakrishna S. J Mater Sci, Mater Med 1999;10:343–52.
[9] Tang ZG, Teoh SH. Coll Surf B: Biointerf 2000;19:19–29.
[10] Carlsson LA. In: Carlsson LA, Pipes RB, editors. Experimental characterization of advanced composite materials. Englewood Cliffs, NJ: Prentice Hall, 1987.
[11] Teoh SH, Tang ZG, Hastings GW. Thermoplastic polymers in biomedical applications: structures, properties, and processing. In: Black J, Hastings GW, editors. Handbook of biomaterials properties. London: Chapman & Hall, 1998. p. 270–302. Chapter 3.
[12] Pienkowski D, Jacob R, Holglin D, Saum K, Kaufer H, Nicholls PJ. J Biomed Mater Res 1995;29:1167–74.
[13] Fu Y, Chen W, Pyda M, Londono D, Annis B, Boller A, Habenschuss A, Cheng J, Wunderlich B. J Macromol Sci, Phys 1996;B35(1):37–87.
[14] Kunz M, Drechsle M, Moller M. Polymer 1995;36(7):1331–9.
[15] Tang ZG. Thin elastomeric composite membranes. PhD Thesis. National University of Singapore; 1999.
[16] Zhu Y, Chang L, Yu S. J Therm Anal 1995;45:329–33.
[17] Zhu QR, Hong KL, Lu F, Qi RR, Pang WM, Zhou GE. Sci China 1995;38(11):1288–96.
[18] Zhu QR, Hong KL, Ji LQ, Qi RR, Zhou GE, Song MS, Wong YW. J Polym Sci B: Polym Phys 1995;33:739–44.